Cell Death and Differentiation (2017) 24, 1772–1783
 1350-9047/17

www.nature.com/cdd

Trophoblast survival signaling during human placentation requires HSP70 activation of MMP2-mediated HBEGF shedding

Chandni V Jain[1,2], Philip Jessmon[2,3], Charbel T Barrak[2], Alan D Bolnick[2], Brian A Kilburn[2], Michael Hertz[2] and D Randall Armant[*,2,3]

Survival of trophoblast cells in the low oxygen environment of human placentation requires metalloproteinase-mediated shedding of HBEGF and downstream signaling. A matrix metalloproteinase (MMP) antibody array and quantitative RT-PCR revealed upregulation of MMP2 post-transcriptionally in human first trimester HTR-8/SVneo trophoblast cells and placental villous explants exposed to 2% O_2. Specific MMP inhibitors established the requirement for MMP2 in HBEGF shedding and upregulation. Because α-amanitin inhibited the upregulation of HBEGF, differentially expressed genes were identified by next-generation sequencing of RNA from trophoblast cells cultured at 2% O_2 for 0, 1, 2 and 4 h. Nine genes, all containing HIF-response elements, were upregulated at 1 h, but only HSPA6 (HSP70B') remained elevated at 2–4 h. The HSP70 chaperone inhibitor VER 155008 blocked upregulation of both MMP2 and HBEGF at 2% O_2, and increased apoptosis. However, both HBEGF upregulation and apoptosis were rescued by exogenous MMP2. Proximity ligation assays demonstrated interactions between HSP70 and MMP2, and between MMP2 and HBEGF, supporting the concept that MMP2-mediated shedding of HBEGF, initiated by HSP70, contributes to trophoblast survival at the low O_2 concentrations encountered during the first trimester, and is essential for successful pregnancy outcomes. Trophoblast survival during human placentation, when oxygenation is minimal, required HSP70 activity, which mediated MMP2 accumulation and the transactivation of anti-apoptotic ERBB signaling by HBEGF shedding.
Cell Death and Differentiation (2017) **24,** 1772–1783; doi:10.1038/cdd.2017.104; published online 21 July 2017

In humans, the placenta is not fully perfused with oxygenated maternal blood until after the tenth week of pregnancy, rendering the implantation site a low (~2%) O_2 environment.[1] Atypical of most cells, human trophoblast (TB) cells survive at low O_2, and proliferate more rapidly.[2] The epidermal growth factor (EGF) family member, heparin-binding EGF-like growth factor (HBEGF), which is highly expressed in the uteroplacental compartment during implantation and placentation,[3] prevents death of human TB cells exposed to low O_2 concentrations.[2] Although HBEGF is upregulated ~100-fold in TB cells after exposure to 2% O_2, HBEGF mRNA remains unchanged (2500 copies/cell).[2] As O_2 increases upon full perfusion of the intravillous space after 10 weeks of gestation,[1] HBEGF positively regulates TB motility and invasion.[3] Survival of TB cells at low (2%) O_2 requires metalloproteinase-mediated shedding of membrane-bound proHBEGF and HBEGF downstream signaling.[2] HBEGF secretion allows activation of ERBB receptor tyrosine kinases, including its cognate receptors, EGF receptor/ERBB1 and ERBB4.[3] During hypoxia, HBEGF is upregulated through an autocrine feedback mechanism that blocks apoptosis through parallel signaling.[2,3] HBEGF activation of ERBB receptor tyrosine kinases prevents apoptosis by activating p38 (MAPK14), while biosynthesis of HBEGF is mediated by any one of the MAPKs, p38, ERK (MAPK1/3) or JNK (MAPK8/9/10), based on experiments using specific inhibitors.[3,4] However, it is unclear whether the MAPKs specifically function downstream of HBEGF, or also operate further upstream in the cascade initiated by hypoxia before proHBEGF shedding. The hypertensive pregnancy disorder, preeclampsia, in which TB invasion is reduced and apoptosis elevated, is characterized by dysregulation of HBEGF and other components of the EGF signaling system.[5,6] Therefore, HBEGF deficiency could contribute to TB dysfunction associated with placental insufficiency disorders.

It is well established that metalloproteinases contribute to invasion and tissue remodeling.[7,8] Implantation and TB invasion are closely linked to expression of matrix metalloproteinases (MMPs).[9] The gelatinases (gelatinase A/MMP2; 72-kDa, and gelatinase B/MMP9; 92-kDa), which target major components of basement membranes (e.g., collagen IV), are expressed by TB cells and key to the invasion process.[9] MMP2 and MMP9 are differentially expressed in first trimester TB cells, with MMP2 more prominently secreted until 9 weeks.[9] MMP2 is constitutively expressed throughout pregnancy, but its activity diminishes in full-term placenta. MMP9 is mainly expressed by TB cells after Week 9, decreasing at term. Thus, MMP2 and MMP9 are expressed and functional throughout the period of O_2 fluctuation in the reproductive tract.[9,10] While their role in tissue remodeling is well known,[7,8] emerging evidence reveals that MMPs, including MMP2 and MMP9, participate in shedding of membrane-anchored

[1]Department of Physiology, Wayne State University School of Medicine, Detroit, MI, USA; [2]Department of Obstetrics and Gynecology, Wayne State University School of Medicine, Detroit, MI, USA and [3]Department of Anatomy and Cell Biology, Wayne State University School of Medicine, Detroit, MI, USA
*Corresponding author: DR Armant, Obstetrics and Gynecology, Wayne State University School of Medicine, Detroit, MI 48201, USA. Tel: +3135771748; Fax: 313-577-8554; E-mail: d.armant@wayne.edu
Received 17.10.16; revised 30.4.17; accepted 19.5.17; Edited by E Baehrecke; published online 21.7.17

signaling molecules.[7,11] Cheng *et al.* reported that bradykinin-induced proliferation of rabbit corneal cells is blocked by an inhibitor of both MMP2 and MMP9, as well as an inhibitor of HBEGF, suggesting that an MMP could contribute to the cleavage of proHBEGF.[12] MMP2 participates in a proteolytic cascade in αT3-1 cells that directs both proHBEGF shedding and EGFR transactivation.[13] In addition, its rapid release in CMTC9 cells after E2 stimulation is correlated with cleavage of proHBEGF.[14] We previously found that treatment with a general metalloproteinase inhibitor blocks HBEGF accumulation in human TB cells at low O_2, causing apoptosis that is rescued with recombinant HBEGF, but not other EGF-like ligands.[2] Autocrine HBEGF activity in TB cells requires, in addition to metalloproteinase-mediated shedding of HBEGF, binding to either EGFR or ERBB4. Blocking HBEGF signaling prevents its upregulation at 2% O_2, suggesting that low levels of resident proHBEGF are cleaved through activation of metalloproteinases to initiate its autocrine accumulation.[2]

Human TB survival at low O_2 is independent of invasion, but equally important for normal placentation. To understand the molecular mechanism of TB survival at low O_2, the HTR-8/SVneo human TB cell line[15] was used. HTR-8/SVneo is an immortalized cell line established from human first trimester cytotrophoblast cells.[15] HTR-8/SVneo cells express the TB epithelial marker cytokeratin (KRT7), as well as the beta subunit of human chorionic gonadotropin (β-hCG), which is TB-specific.[16] This cell line possesses the ability to invade Matrigel basement membrane without tumorigenicity, and expresses the TB-specific major histocompatibility protein, HLA-G, when induced by Matrigel to differentiate.[16] In response to Matrigel, HTR-8/SVneo cells switch integrin expression[3] in association with invasive differentiation, while in response to hypoxia, proliferation increases and extravillous differentiation is inhibited.[16] To examine the hypothesis that MMPs contribute to the shedding and upregulation of HBEGF required for TB survival at the low O_2 concentrations encountered in the first trimester, we used HTR-8/SVneo human TB cells, and conducted confirmatory experiments with human first trimester villous explants.[17,18]

Results

Upregulation of MMP2 at low O_2. Using a human MMP antibody array, we observed that relative expression of MMP2, but not MMP9 or other MMPs, increased 1.7-fold in HTR-8/SVneo TB cells cultured for 4 h at 2% O_2 (Figure 1a), compared with TB cells cultured at 20% O_2. The specific increase in expression of MMP2, and not MMP9, was confirmed by western blotting (Figure 1b). Comparison to recombinant MMP2 and MMP9 zymogens indicated that MMP2 in TB lysates was active, based on its lower molecular weight. Cellular MMP2 was quantified temporally by ELISA after shifting TB cells to 2% O_2. The MMP2 concentration abruptly increased 164-fold ($P<0.0001$) after 2 h at 2% O_2 (Figure 1c), which is 2 h before HBEGF upregulation.[2] MMP2 expression was homogenous throughout the TB cell culture at 2% O_2, similar to HBEGF expression (Supplementary Figure 1B).

Role of MMP2 in HBEGF upregulation. To determine whether MMP2 has a functional role in HBEGF regulation by O_2, specific inhibitors of MMP2 and MMP9 were supplemented in culture medium during manipulation of O_2. HBEGF failed to accumulate in TB cells cultured at 2% O_2 for 4 h when MMP2 was inhibited (Figure 1d). However, MMP9 inhibition had no effect on HBEGF accumulation at low O_2. A third inhibitor that targets both MMP2 and MMP9 also inhibited HBEGF accumulation. Additionally, terminal deoxynucleotidyl transferase-mediated dUTP nick end labeling (TUNEL) showed increased ($P<0.0001$) TB cell death when both MMP2 and MMP9, or only MMP2, were inhibited (Figure 1e), while MMP9 inhibition produced no apoptosis at low O_2. We conclude that MMP2, but not MMP9, either directly or indirectly mediates the proteolytic cleavage of proHBEGF, and subsequent survival signaling.

Role of MAPKs in MMP2 upregulation. We previously showed that upregulation of HBEGF at low O_2 requires MAPK signaling.[4] MMP2 was quantified by ELISA in extracts of TB cells cultured at 2% O_2 for 4 h, with or without specific inhibitors of ERK, p38 and JNK, or the corresponding inactive structural analogs (Table 1). Inhibitors of MAPKs had no effect on the increased MMP2 expression at 2% O_2.

MMP2 mRNA expression. To determine whether MMP2 is transcriptionally upregulated at low O_2, its expression was quantified by qPCR, using RNA extracted from HTR-8/SVneo cells cultured at 20% and 2% O_2 for 1–4 h. Expression values, normalized to GAPDH, were calculated for both MMP2 (Figure 2a) and HBEGF (Figure 2b). MMP2 mRNA, like HBEGF message, did not change ($P=0.8$) at 2% O_2, suggesting that their proteins are both regulated post-transcriptionally.

Role of transcription in HBEGF upregulation. TB cells were cultured at 2% O_2 with or without α-amanitin, an inhibitor of RNA polymerase-II,[19] to examine the role of *de novo* transcription in the upregulation of HBEGF. Cells were pre-incubated with α-amanitin for 3 h to allow complete inhibition of transcription before exposure to 2% O_2. Elevation of HBEGF protein after culture at 2% O_2 for 6 h was abrogated in a dose-dependent manner by α-amanitin, with maximal inhibition attained at 5 μg/ml (Figure 2c). ELISA demonstrated that addition of rMMP2 increased ($P<0.0001$) HBEGF at 20% O_2 to the same extent as TB culture at 2% O_2 (Figure 2d). Furthermore, addition of rMMP2 rescued ($P<0.0001$) HBEGF biosynthesis in the presence of α-amanitin at 2% O_2 (Figure 2d), suggesting that MMP2 accumulates due to hypoxia-induced transcription. It also demonstrates that sufficient amounts of HBEGF mRNA remain after α-amanitin treatment for biosynthesis of HBEGF.

Identification of differentially expressed transcripts. Transcripts differentially expressed in TB cells at the two O_2 concentrations were identified, using a non-biased transcriptomics approach. RNA-seq analysis revealed a total of 9 upregulated (Table 2) and 120 downregulated genes (Supplementary Table 1) after 1 h of exposure to 2% O_2 (Figure 3a). We focused on upregulated genes, based on the effects of α-amanitin inhibition at 2% O_2. HSPA6 was most

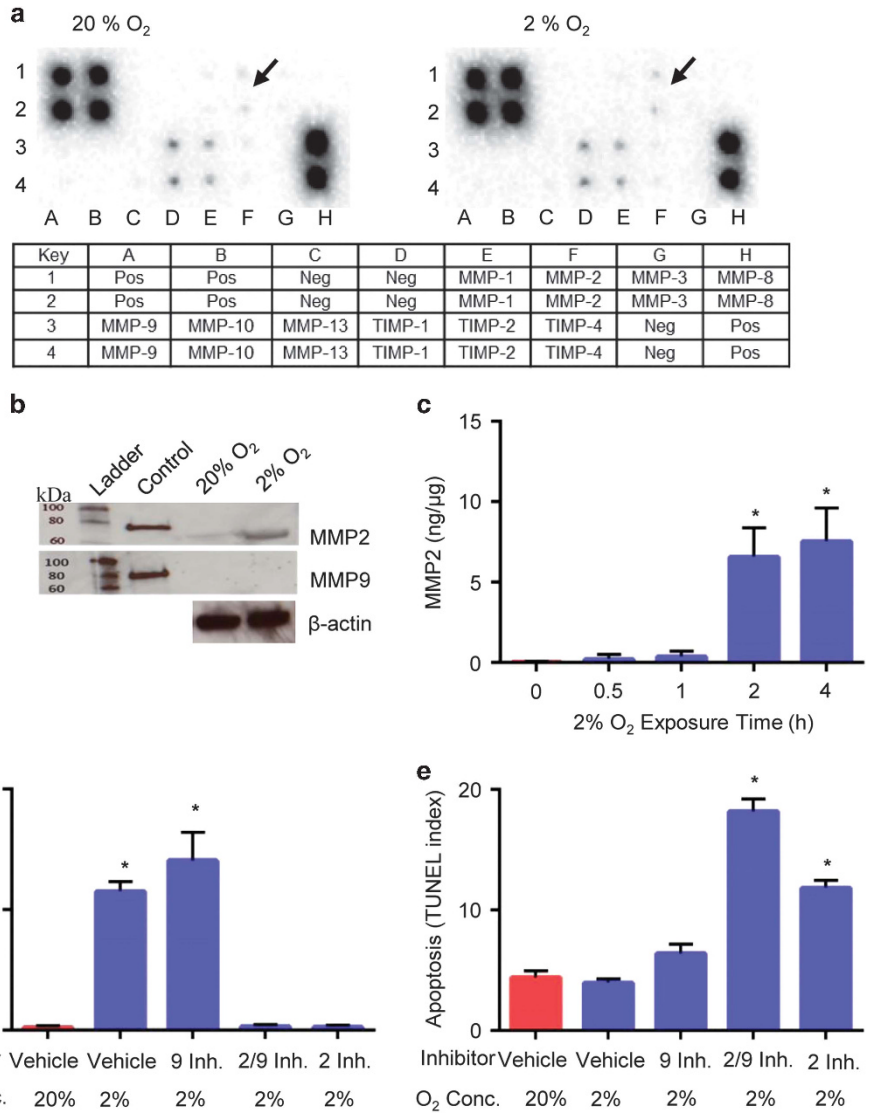

Key	A	B	C	D	E	F	G	H
1	Pos	Pos	Neg	Neg	MMP-1	MMP-2	MMP-3	MMP-8
2	Pos	Pos	Neg	Neg	MMP-1	MMP-2	MMP-3	MMP-8
3	MMP-9	MMP-10	MMP-13	TIMP-1	TIMP-2	TIMP-4	Neg	Pos
4	MMP-9	MMP-10	MMP-13	TIMP-1	TIMP-2	TIMP-4	Neg	Pos

Figure 1 Upregulation of MMP2 at low O_2, and its effects on HBEGF and cell survival. (**a**) Expression arrays for MMP-related proteins incubated with extracts of HTR-8/SVneo cells cultured at 20% (left) or 2% (right) O_2. Arrows indicate elevated MMP2 at 2% compared with 20% O_2. The key below indicates the location of duplicate antibody probes for each protein according to the coordinates shown, including both positive (Pos) and Negative (Neg) controls. (**b**) Western blots of molecular weight standards (Ladder), recombinant proMMP2 or proMMP9 zymogens (Control), and extracts of TB cells cultured at 20% or 2% O_2, as indicated. The upper blot was labeled with anti-MMP2, the middle blot was labeled with anti-MMP9, and lower blot was labeled with anti-β-actin. (**c**) MMP2 quantified by ELISA in TB cells cultured 0–4 h at 2% O_2. (**d**) HBEGF quantified by ELISA in TB cells treated during culture for 4 h with the indicated MMP inhibitor or vehicle, and concentration of O_2. (**e**) Apoptosis was quantified in TB cells cultured as in D using the TUNEL assay. $^*P<0.05$, compared with the control (0 h, vehicle/20% O_2), $n=3$

upregulated (870-fold) (Table 2), and the only gene that remained elevated at 2–4 h (Figures 3b and c). Elevated HSPA6 expression at 2% O_2 was validated using qPCR (18-fold, $P<0.0001$) and western blotting (2.3 fold, $P<0.05$) (Figures 3d and e). Additionally, the homogenous increase in expression of HSPA6 at 2% O_2 was validated in the HTR-8/SVneo cell line (Supplementary Figure 1B). Extraction of the promoter region revealed two overlapping hypoxia response elements (HREs) 2.4 kb upstream of the 5′-most HSPA6 transcriptional start site (Supplementary Figure 2).

$CoCl_2$ and HBEGF upregulation. $CoCl_2$, a hypoxia mimetic that stabilizes hypoxia inducible factor (HIF),[20] was examined for its effect on HBEGF. At 20% O_2, $CoCl_2$ increased ($P<0.0001$) HBEGF levels. As expected, $CoCl_2$ induced accumulation of HIF1A and HIF2A, comparable to the effect of low O_2, according to western blotting (Figure 4a; Supplementary Figures 3A and B). The $CoCl_2$-induced accumulation of HIF1A (Figure 4b) and HIF2A (Figure 4c) was quantified by ELISA, establishing significant increases. α-Amanitin blocked the $CoCl_2$-mediated increase in HBEGF (Figure 4d), suggesting that transcription of HIF-regulated genes initiate MMP2 accumulation and HBEGF shedding. However, HIF1A and HIF2A were not homogenously expressed by cells at low O_2 (Supplementary Figure 3D) and thus might not be essential for HBEGF upregulation.

HIFs and HBEGF upregulation. HIF1A and HIF2A were both knocked down in HTR-8/SVneo cells by transfection for 48 h with specific siRNAs. Controls included no treatment and transfection with scrambled siRNA. Culture was continued for 4 h at either 20% O_2 or 2% O_2. HIF1A and HIF2A were greatly reduced in cells transfected with 50 pM of the targeting siRNA, but not in control treatments, as quantified by ELISA (Figures 5a and b). The lack of cross reactivity between HIF1A and HIF2A was determined by ELISA using either HIF1A antibody or HIF2A antibody against HIF1A peptide or HIF2A peptide (Supplementary Figures 4A and B). Lysates were assayed either by western blot or ELISA to verify expression of HSPA6, MMP2 and HBEGF. It was observed that knockdown of HIF1A and HIF2A at 2% O_2 prevented the upregulation (2.4 fold) of HSPA6, (1.3 fold, $P<0.05$; Figure 5c). However, HIF knockdown did not prevent upregulation of MMP2 and HBEGF at 2% O_2 (Figures 5d and e). MMP2 levels approximated 0.01 ng/μg at 20% O_2, and rose to 15 ng/μg (range 18.8–14.2 ng/μg) at 2% O_2 in all controls and transfected cells (Figure 5d).

Table 1 MMP2 upregulation is independent of MAPKs

% O_2	Treatment	MMP2 (ng/ml)
20	Vehicle	0.03 ± 0.03
2	Vehicle	7.27 ± 0.74*
2	U 0126/ERK inhibitor	6.07 ± 0.55*
2	U0124/ERK negative control	7.40 ± 0.66*
2	JNK inhibitor	5.44 ± 1.98*
2	JNK negative control	6.53 ± 1.23*
2	SB203580 P38 inhibitor	6.17 ± 0.87*
2	SB 202474 P38 negative control	7.15 ± 0.89*
2	All 3 inhibitors	5.86 ± 1.51*
2	All 3 neg. controls	6.34 ± 0.68*

*$P<0.0001$

Table 2 Upregulated transcripts from RNA-Seq analysis

Gene symbol	Gene ID	Log 2 fold change		
		0 h *versus* 1 h	0 h *versus* 2 h	0 h *versus* 4 h
HSPA6	3310	6.771	7.78	6.55
FAP	2191	5.188	—	—
LOC100131607	100131607	5.043	—	—
SNORA5A	654319	4.826	—	—
RPS16P5	647190	4.794	—	—
ZNF319	57567	4.564	—	—
IL8	3576	4.435	—	—
VTRNA1-3	56662	4.039	—	—
CLK1	1195	3.687	—	—

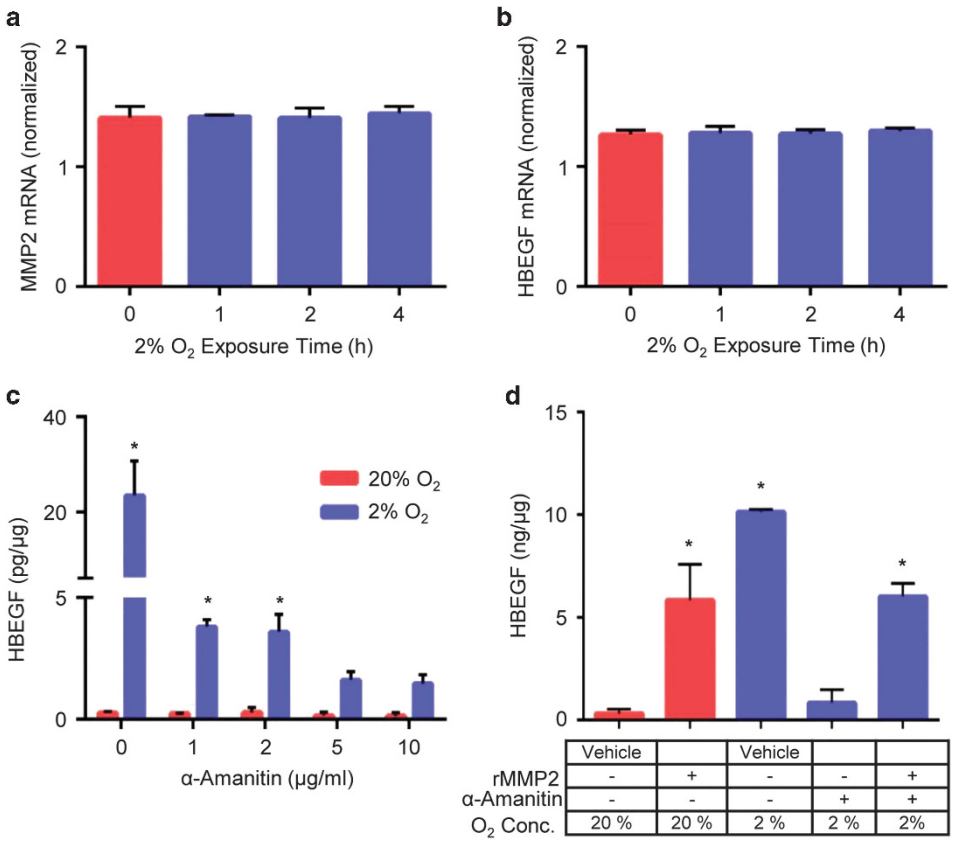

Figure 2 Expression of MMP2 and HBEGF at 2% O_2 in HTR-8/SVneo cells. MMP2 (**a**) and HBEGF (**b**) mRNA were measured by qPCR after culture for indicated time at 2% O_2. HBEGF protein measured by ELISA in extracts of TB cells cultured at the indicated concentrations of α-amanitin and O_2 (**c**) and in cellular extracts of TB cells cultured for 4 h at either 20% or 2% O_2 in the presence of 10 nM recombinant MMP2 (rMMP2) and α-amanitin, as indicated (**d**). *$P<0.05$, compared with no treatment/vehicle/20% O_2, $n=3$

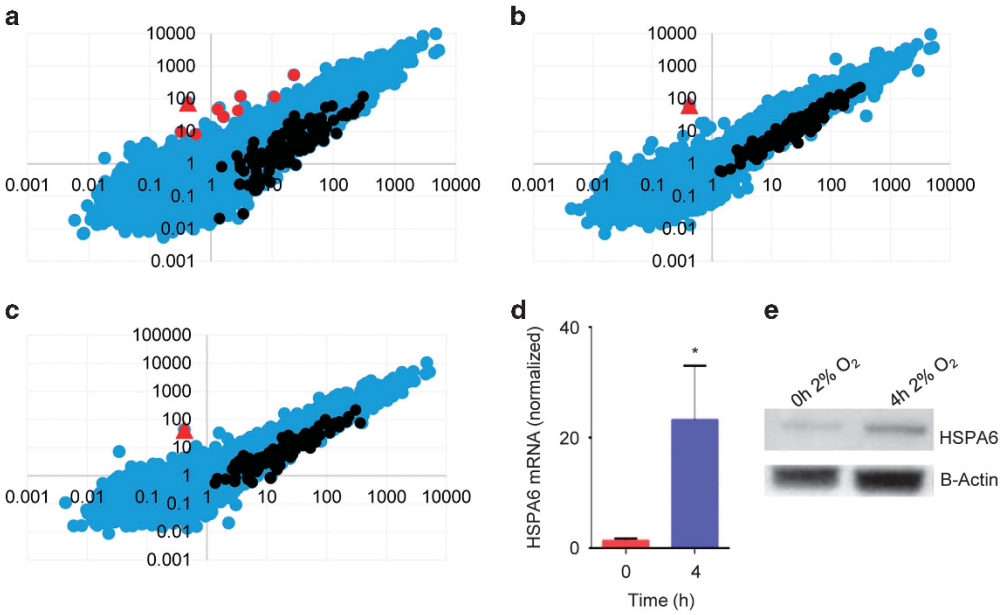

Figure 3 Transcriptome analysis of HTR-8/SVneo cells exposed to 2% O_2. (**a–c**) Abundance of transcripts compared using GGA workstation between cells cultured at 2% O_2 for 0 h (*x*-axis) and 1 h (**a**, *y*-axis), 2 h (**b**, *y*-axis) or 4 h (**c**, *y*-axis). Unchanged transcripts are indicated in blue, upregulated transcripts are red, and downregulated transcripts are black. HSPA6 (red triangle) was the most highly upregulated mRNA, and only transcript upregulated at 2 h and 4 h. (**d**) HSPA6 mRNA was measured by qPCR in TB cells cultured for indicated time at 2% O_2. (**e**) Western blots of HSPA6 (~70 kDa) and β-actin (~43 kDa) in lysates of TB cells cultured for indicated time at 2% O_2

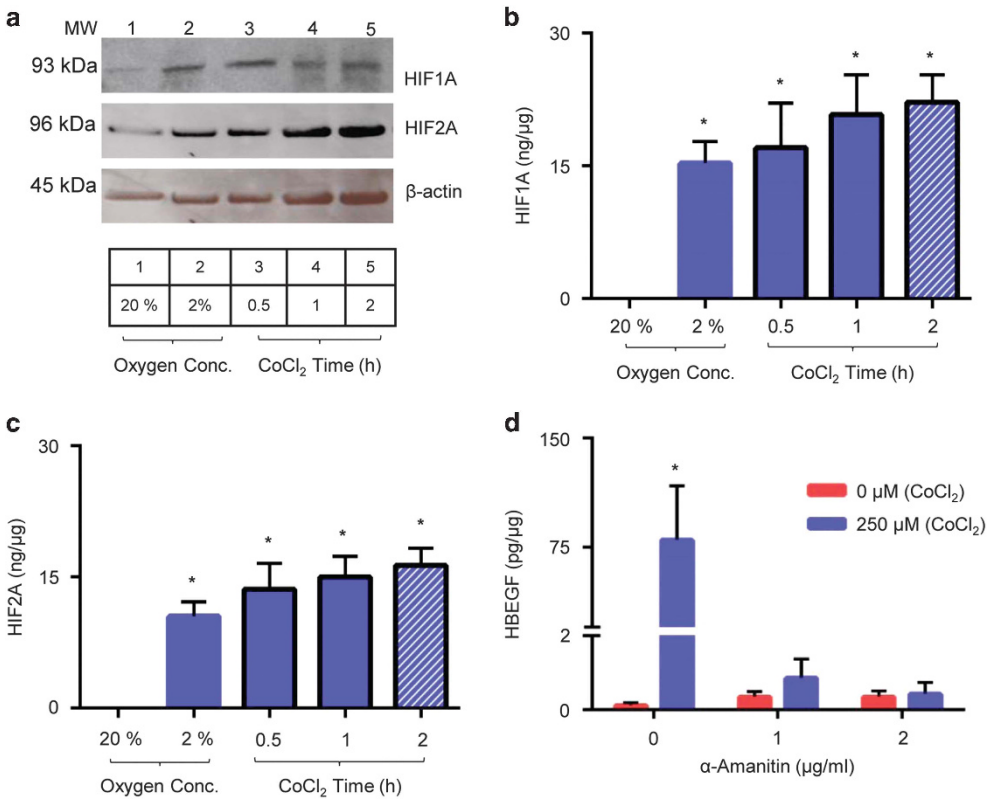

Figure 4 Expression of HBEGF in presence of $CoCl_2$ in HTR-8/SVneo cells. (**a**) Western blots of HIF1A (~ 93 kDa), HIF2A (~96 kDa) and β-actin (~45 kDa) in lysates of TB cells treated at 20% O_2 or 2% O_2 for 4 h, or at 20% O_2 in the presence of 250 μM $CoCl_2$ for 0.5–2 h, as indicated in the key below gel images. HIF1A (**b**) and HIF2A (**c**) proteins measured by ELISA in extracts of TB cells treated at 20% O_2 or 2% O_2 for 4 h, or at 20% O_2 in the presence of 250 μM $CoCl_2$ for 0.5–2 h. (**d**) HBEGF protein measured by ELISA in extracts of TB cells cultured at the indicated concentrations of α-amanitin and $CoCl_2$ at 20% O_2. $^*P<0.05$ compared with no treatment control, $n=3$

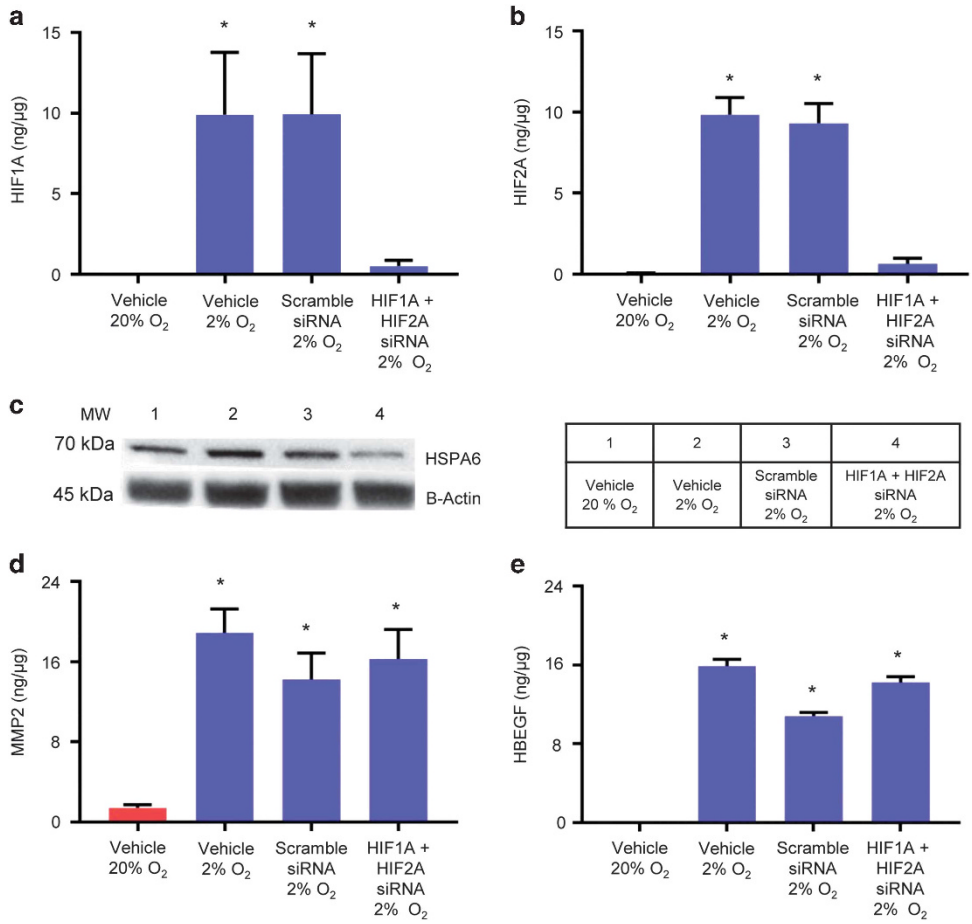

Figure 5 Effect of HIF1A and HIF2A knockdown on regulation of HBEGF by O_2. HIF1A (**a**) and HIF2A (**b**) protein measured by ELISA in extracts of HTR-8/SVneo cells cultured for 48 h at 20% O_2, with or without 50 pM of either scrambled siRNA or siRNA for HIF1A and HIF2A. Afterwards, culture was continued for 4 h at 20% O_2, or at 2% O_2 with vehicle, scrambled siRNA or siRNA for HIF1A and HIF2A, as indicated. (**c**) Lysates of TB cells treated as in (**a** and **b**) (key on right) were assayed by western blot for HSPA6 (70 kDa) and β-actin (45 kDa). MMP2 (**d**) and HBEGF (**e**) ELISAs with lysates of TB cells treated as in a and b.*, $P<0.005$, compared with control (Vehicle 20% O_2), $n=3$

HBEGF was not expressed at 20% O_2, and rose to 13.3 ng/μg (range 15.8–10.8 ng/μg) at 2% O_2 in all controls and transfected cells (Figure 5e). Therefore, in the absence of HIF and HSPA6 upregulation, O_2 continued to regulate MMP2 and HBEGF.

HSP70 function in MMP2 and HBEGF upregulation. Inhibition of HSP70 with a pharmacological inhibitor, VER 155008,[21] caused a dose-dependent decrease in MMP2 (Figure 6a) and HBEGF (Figure 6b) in TB cells cultured at 2% O_2, demonstrating a functional role for HSPA6 (HSP70B').[22] TUNEL assays showed increased ($P<0.0001$) TB cell death with HSP70 inhibition (Figure 6c), suggesting that survival at 2% O_2 requires HSPA6 activity. rMMP2 increased ($P<0.0001$) HBEGF at 20% O_2 (Figure 6d), and rescued ($P<0.0001$) HBEGF biosynthesis in the presence of HSP70 inhibitor at 2% O_2 (Figure 6d). Therefore, upregulation of MMP2 requires HSPA6 activity, while upregulation of HBEGF requires only shedding mediated by MMP2.

Regulation of MMP2 in placental explants. Using immunocytochemistry and ELISA, we confirmed the observed increase in MMP2, using first trimester villous explants cultured at 8% or 2% O_2 (Figures 7a and b). Furthermore, it was confirmed that HSP70 inhibitor prevents the upregulation of MMP2 (Figures 7a and b) and HBEGF (Figures 7c and d). Both MMP2 and HBEGF were most prominently expressed in the TB. rMMP2 increased ($P<0.0001$) HBEGF at 8% O_2, and rescued ($P<0.0001$) HBEGF upregulation at 2% O_2 during treatment with HSP70 inhibitor (Figures 7c and d). TUNEL showed increased ($P<0.05$) cell death during HSP70 inhibition at 2% O_2 that was rescued ($P<0.05$) by rMMP2 (Figures 7e and f), suggesting that survival at 2% O_2 requires HSPA6 activity.

Interaction of key regulators of survival signaling. Our findings suggest that HSPA6, MMP2 and HBEGF interact to initiate HBEGF upregulation and inhibition of apoptosis in TB cells exposed to 2% O_2. Proximity ligation assays (PLA) were used to determine whether these proteins physically interact at 2% O_2. Examining confluent fields of TB cells (Figures 8a–d, upper panels, DAPI) interactions were identified between HSPA6 and MMP2, MMP2 and HBEGF, but not between HSPA6 and HBEGF, or control cells treated with

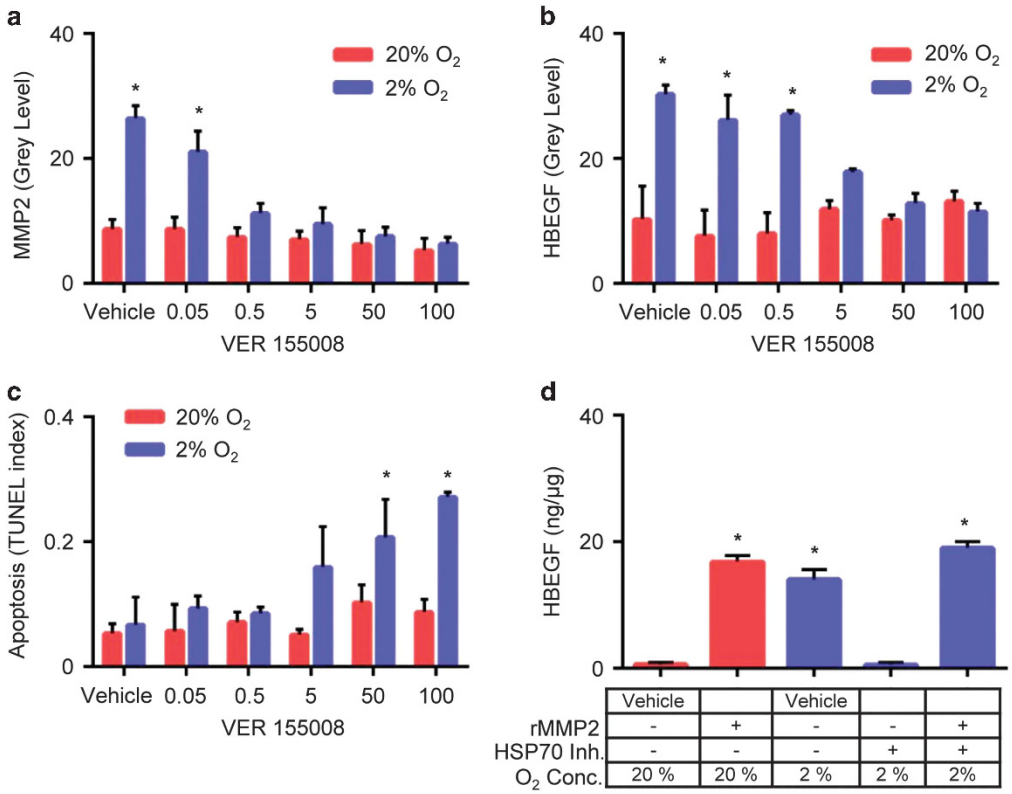

Figure 6 Regulation of MMP2, HBEGF and cell survival by HSP70. HSP70 was inhibited using the pharmacological inhibitor VER 155008 during culture of HTR-8/SVneo cells for 4 h at 20% or 2% O_2. At 2% O_2, HSP70 inhibition caused a dose-dependent decrease in both MMP2 (**a**) and HBEGF (**b**), measured by immunohistochemistry, and concomitantly increased cell death (**c**), measured by TUNEL. Cells cultured at 20% O_2 were unaffected. (**d**) ELISA for HBEGF in cellular extracts of TB cells cultured for 4 h at either 20% or 2% O_2 in the presence of 10 nM recombinant MMP2 (rMMP2) and 5 μM HSP70 inhibitor (VER 155008), as indicated. *$P<0.05$, compared with vehicle/20% O_2, $n=3$

non-immune primary antibody (Figures 8a–d, lower panels, red PLA signal). These results confirm our experimental findings that HSPA6 mediates upregulation of MMP2, and suggest a direct interaction. Furthermore, PLA results indicated that MMP2 could be the sheddase for HBEGF. Based on these findings, a mechanism is proposed for HBEGF shedding in response to low O_2 (Figure 9).

Discussion

The regulation of HBEGF signaling during implantation and placentation is critical for TB survival and invasion.[3] An autocrine, post-transcriptional mechanism induced at low O_2 upregulates HBEGF synthesis and secretion, providing an important survival factor during early gestation.[2,3] Evidence suggests that autocrine signaling is initiated by metalloproteinase-mediated shedding of proHBEGF.[2] In seeking a metalloproteinase responsible for HBEGF shedding, a human MMP antibody array, verified by western blot and ELISA, implicated proteolysis by MMP2. A functional role for MMP2 in the accumulation of HBEGF and cell survival was established using a specific inhibitor. However, MMP2 mRNA concentration was unaltered by reduced O_2, suggesting that it was regulated post-transcriptionally. Interestingly, very low O_2 (0.1%) increases MMP2 mRNA levels 1.7-fold in TB cells isolated from first trimester placentas,[23] which was not found in our study. However, culture at 2% O_2 could differ significantly from 0.1% O_2, and account for the different outcomes. Transcriptomic analysis identified HSPA6, a member of the HSP70 family, as a potential regulator upstream of MMP2. Using an inhibitor of HSP70 and exogenous rMMP2, evidence was obtained supporting a mechanism wherein low O_2 concentrations encountered by TB cells during the first 10 weeks of placentation induce transcription of HSP70, a chaperone that directly or indirectly facilitates MMP2 accumulation, likely through physical interaction (Figure 8b). MMP2, in turn, mediates HBEGF shedding.[7,13] It remains uncertain whether other metalloproteinases that activate the HBEGF sheddase are co-regulated with MMP2. However, PLA suggested that MMP2 and HBEGF interact (Figure 8d), supporting a role for MMP2 as the HBEGF sheddase. The secretion of HBEGF initiates autocrine signaling through its cognate receptors, EGFR and ERBB4, mobilizing biosynthesis from constitutively expressed, but latent, HBEGF mRNA (Figure 9). We recently proposed that HBEGF signaling activates translation from HBEGF mRNA through interactions of microRNA with its 3′ untranslated region.[24]

HBEGF regulates TB survival and invasion, two crucial functions that are compromised in pregnancies complicated by preeclampsia.[25,26] Supplementation with HBEGF and other EGF family members, including EGF or TGFα, has little effect on proliferation, but is highly effective at converting TB cells to

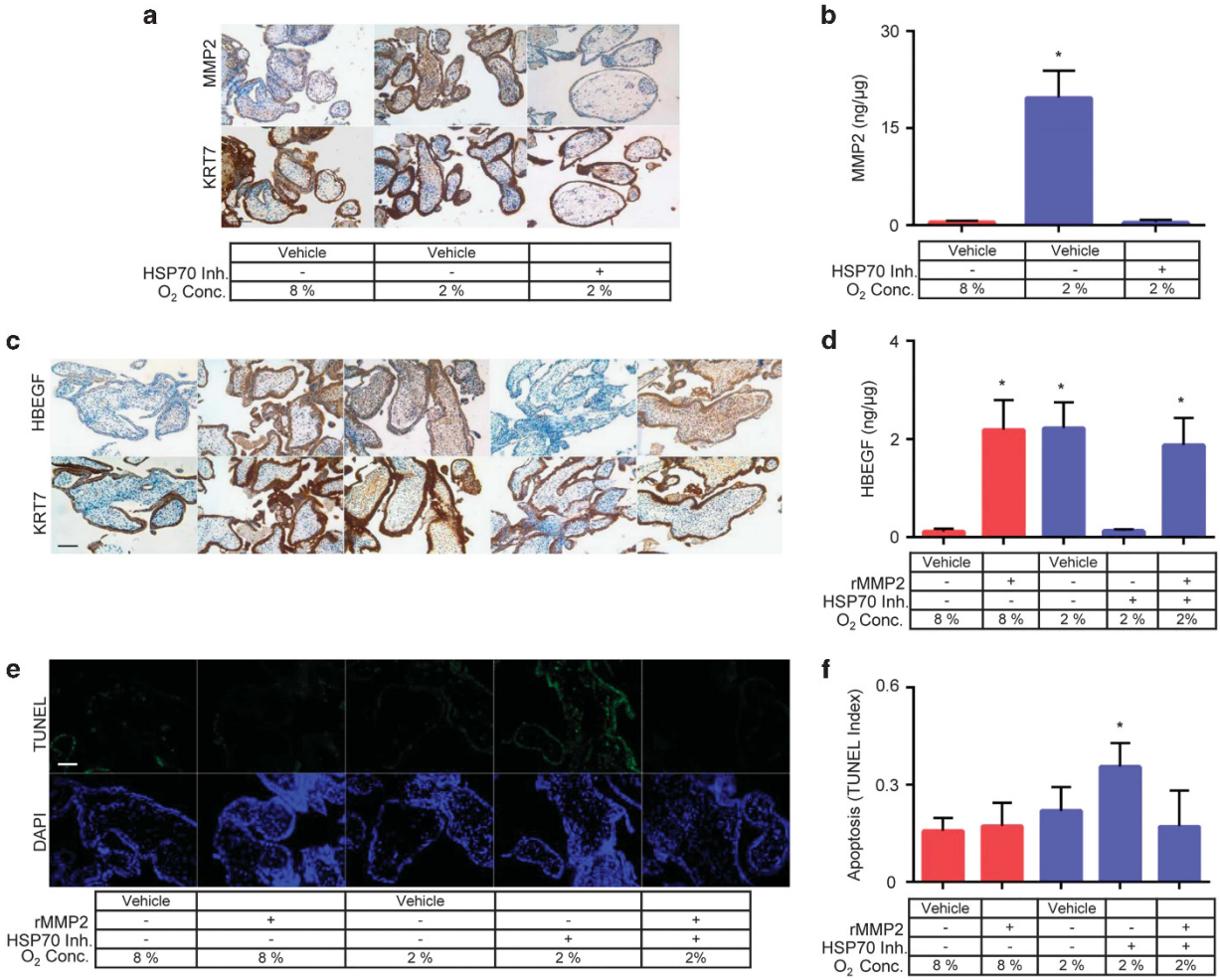

Figure 7 Regulation of MMP2 in first trimester chorionic villous explants. First trimester villous explants cultured for 6 h at either 8% or 2% O_2 in the presence of recombinant MMP2 (rMMP2) and VER 155008 (HSP70 inh.), as indicated, were stained for MMP2 & RT7 (**a**), HBEGF &RT7 (**c**) and counterstained with Hematoxylin (blue). Cell extracts were assayed by ELISA for MMP2 (**b**) and HBEGF (**d**) Sections of villous explants were dual stained with DAPI and TUNEL (**e**), using immunofluorescence microscopy and quantified for apoptosis (**f**). Size bars in **a** and **c** indicate 10 μm, and in (**e**) indicate 100 μm. *$P<0.0001$ in (**b** and **d**), $P<0.05$ in (**f**), compared with vehicle/8% O_2, $n=3$

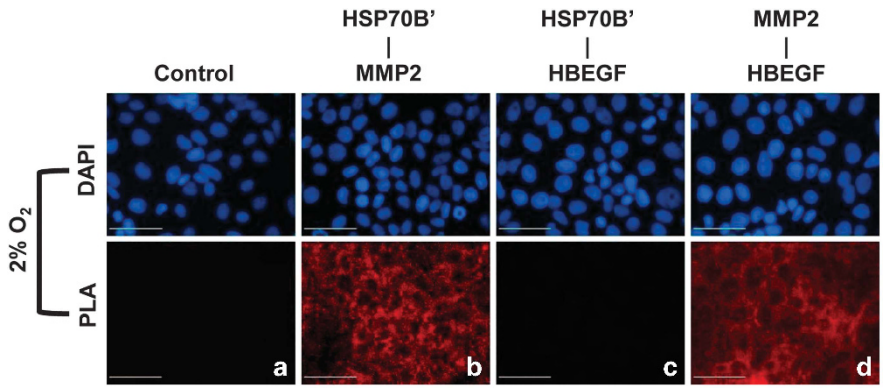

Figure 8 Proximity ligation assay (PLA) for protein interactions during survival signaling. HTR-8/SVneo cells were cultured at 2% O_2 for 4 h and duo labeled with non-immune IgG (**a**) or combinations of antibodies against HSPA6 (HSP70B′), MMP2 and HBEGF (**b**–**d**, as indicated). Cell nuclei were stained with DAPI (blue), and positive interactions between the indicated proteins in (**b**–**d**) are labeled red (PLA signal). Size bars indicate 50 μm

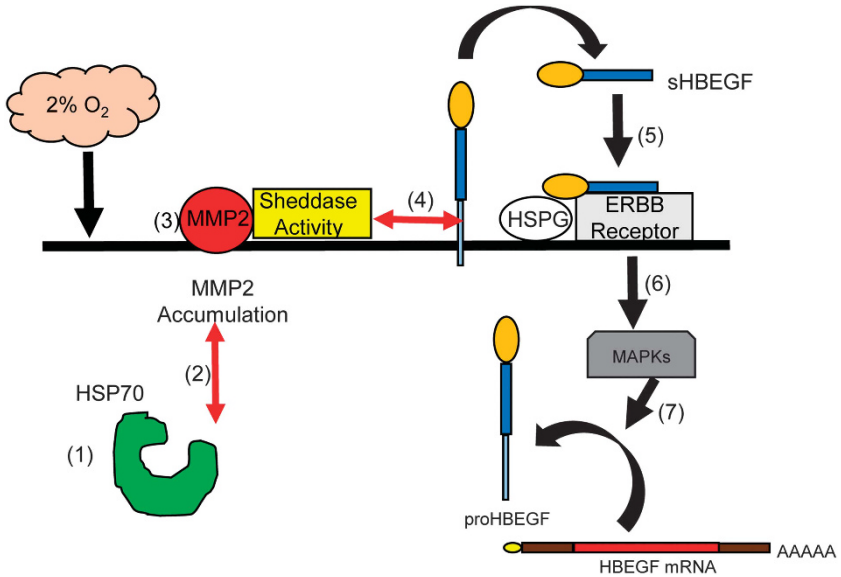

Figure 9 Proposed mechanism for regulation of HBEGF by O_2. Low (2%) O_2 upregulates HSP70 (1). HSP70 interacts with MMP2 (2) and regulates the accumulation of activated MMP2 at the cell surface (3), where it interacts with proHBEGF (4) possibly as its sheddase. The released sHBEGF binds (5) to its receptors, ERBB1 and ERBB4, through its EGF-like domain, and to heparan sulfate proteoglycans (HSPG) through its heparin-binding domain. ERBB downstream signaling activates MAPKs (6) required for biosynthesis of proHBEGF from the pool of HBEGF mRNA (7). HBEGF autocrine signaling thereby increases HBEGF secretion to achieve extracellular HBEGF concentrations (>1 nM) sufficient to inhibit apoptosis at 2% O_2. Red arrows indicated that a direct interaction was demonstrated using proximity ligation assays

an invasive phenotype.[3] The extensive expression of HBEGF by TB cells, particularly within extravillous populations,[5] could be vital for their invasive activities during the establishment of pregnancy and physiological conversion of spiral arteries. Accordingly, HBEGF and other components of the EGF signaling system are disrupted in placentas of women with preeclampsia.[5,6] The increased oxidative damage to TB cells[27] and the decrease in HBEGF in preeclamptic placentas is consistent with the hypothesis that HBEGF is an important survival factor throughout gestation.

Jessmon *et al*. showed that HBEGF activates ERK, p38 and JNK in human TB cells, while treatment with specific inhibitors indicated that hypoxia upregulates HBEGF biosynthesis through any one of the three examined MAPKs.[2,3] However, it was unclear whether this MAPK pathway was functional upstream or downstream of HBEGF shedding. Therefore, MMP2 was quantified in human TB cells cultured at 2% O_2 with specific inhibitors of ERK, p38 and JNK. These inhibitors did not influence the upregulation of MMP2 at low O_2, suggesting that the MAPKs function exclusively downstream of HBEGF signaling through the ERBB1/4 tyrosine kinases in human TB cells, as indicated in Figure 9.

Although both MMP2 and HBEGF are regulated by O_2 post-transcriptionally, HBEGF upregulation by low O_2 or $CoCl_2$ was blocked by *α*-amanitin, suggesting the requirement for transcription of other genes that regulate HBEGF. The transcriptome was analyzed as TB were exposed to 2% O_2, which revealed HSPA6/HSP70B′ as the most highly upregulated gene at 1–4 h. Extraction of the HSPA6 promoter revealed two overlapping HREs on the sense and anti-sense strands. HREs also appeared in the promoters of eight other mRNAs that increased 1 h after exposure to low O_2. The presence of HREs in all upregulated genes suggested a potential role for HIFs. HIF proteins are stabilized at low O_2,[28] and activate transcription of targeted genes by interaction with specific HREs in the gene promoters,[29] along with transcriptional coactivators, to form an initiation complex.[30] We suspected that either HIF1A or HIF2A could be involved in the response of TB cells to low O_2, based on their accumulation under the influence of $CoCl_2$ or 2% O_2, which was previously reported in JEG3 choriocarcinoma cells.[31] Knockdown of HIF1A and HIF2A was without effect, which suggested that HIF's are not essential for the upregulation of HBEGF. However, residual levels of HIFs might have been adequate to maintain function. An inhibitor of HIFs is not currently available.

Induction of heat shock proteins (HSPs) in response to cellular stress has been proposed as a potential strategy of eukaryotic cells to combat lethal conditions.[32] Within the HSP family, HSP70 functions in the recovery of cells from stress, and in guarding against further insults.[33] HSP70 is a multigene family that includes the stress-inducible members HSPA6 and HSPA1A/HSP70-1.[22,34] HSP70 forms a molecular chaperone complex with HSP90, another highly conserved and essential HSP family member.[35,36] This molecular chaperone complex is dependent on the hydrolysis of ATP, and ADP/ATP exchange, and is mediated by association with HOP (Hsp70/Hsp90-organizing protein)/STIP1 (stress-induced phosphoprotein 1).[37] The HSP70/HSP90 molecular chaperone complex, optimized by HOP, coordinates interactions that ensure folding and conformational regulation of proteins under stress.[38,39] RNAi knockdown of HOP in pancreatic cancer cells decreases MMP2 expression.[40] Additionally, inhibition or depletion of HSP70 in the breast cancer cell line, MA-MB-231, decreases cell migration and invasion due to a lack of MMP2 activation.[41] This suggests that molecular relationships

between HSPs, various signaling proteins, and partner proteins mediate the integrity of signal transduction pathways.[42] Our findings further support the role for HSP70 in mediating MMP2 function through direct interaction.

The signaling cascade delineated in the present study (Figure 9) could influence multiple physiological processes that have a key role in placentation. MMP2 belongs to a family of extracellular matrix-remodeling enzymes that have been implicated in the regulation of vasculogenesis, which is disrupted in placental insufficiency disorders, including pre-eclampsia. There is compelling evidence that MMP2, but not MMP9, increases in women who subsequently develop preeclampsia.[43–46] HSP70 also appears to be altered in adverse pregnancies. In a pilot study, higher levels of HSP70 were reported in patients with early onset of severe PE.[47,48] Fukushima *et al.* reported that serum levels of HSP70 are constant throughout normal pregnancy, but increase significantly in women with preeclampsia or preterm delivery.[49] Increased circulating HSP70 in preeclamptic patients could arise from systemic inflammation caused by disease and oxidative stress.[50,51] In term preeclamptic placentas, HIF1A and HSP70 are both elevated and localize prominently in syncytiotrophoblasts and villous endothelial cells.[31] In another study of HSP70 in term placentas, both mRNA and protein increased in women with preeclampsia and intrauterine growth restriction.[52] However, there has been no information reported on the expression or role of placental HSP70 in the first trimester before this study.

Using a human TB cell line and a villous explant model, we have established a role for HSPA6 (HSP70B′) in the regulation of MMP2 biosynthesis, which is required for HBEGF shedding at low O_2. These findings suggest that TB survival in the low O_2 environment during early pregnancy requires this signaling pathway. Disruption of any component during the first trimester could compromise TB survival and function, leading to placental insufficiency and the resulting obstetrical complications of pregnancy.

Materials and Methods

Cell culture and treatments. The first trimester human TB cell line, HTR-8/SVneo,[15] were grown in either 96-well culture plates (~500 000 cells) or T25 tissue culture flasks (~85% confluency) and cultured during experiments in sterile DMEM/F-12 with 1 mg/ml BSA at either 20% O_2 or 2% O_2. Cells were treated by adding to the culture medium 1–10 μg/ml α-amanitin (Sigma-Aldrich, St. Louis, USA) (3 h pretreatment with α-amanitin), 250 μM $CoCl_2$ (Sigma-Aldrich), inhibitors (EDM Chemicals, Inc., Gibbstown, NJ, USA) specific for MMP2 and MMP9 ((2R)-[(4-Biphenylylsulfonyl)amino]-N-hydroxy-3-phenylpropionamide, BiPS; 100 nM),[53] MMP2 only ((2-((isopropoxy)-(1,1′-biphenyl-4-ylsulfonyl)-amino))-N-hydroxyacetamide; 250 nM)[54] or MMP9 only (MMP9 Inhibitor I; 100 nM),[55] specific inhibitors for ERK, JNK, and p38,[4] HSP70 inhibitor (VER 155008, Santa-Cruz Biotech, Dallas, TX, USA; 0.05–100 μM), and 10 nM recombinant MMP2 (R&D Systems, Minneapolis, MN, USA; rMMP2). For protein analysis attached cells were extracted using cell lysis buffer (Cell Signaling, Beverly, MA, USA) and total cellular protein concentrations were determined using Pierce BCA protein assay kit (ThermoFisher Scientific, Waltham, MA, USA). The HTR-8/SVneo cell line was maintained in DMEM/F-12 with 10% donor calf serum at 20% O_2 between passages 30–50, and routinely checked for homogeneous production of β-hCG, KRT7, and when cultured on Matrigel, HLA-G. Serum was replaced with BSA beginning 24 h before all experiments.

Villous explant culture. Placental tissues were obtained with Wayne State University Institutional Review Board approval and patient informed consent from first trimester terminations at a Michigan family planning facility. Fresh tissue was placed on ice in PBS and immediately transported to the laboratory. The chorionic villi were dissected into pieces of ~ 5 mg wet weight and transferred individually into DMEM/F-12 culture medium supplemented with 10% donor calf serum, 100 I.U. penicillin and 100 μg/ml streptomycin in a 24-well culture plate (Costar, Corning, NY, USA) for villous explant culture.[56] Treatments were performed as described for the cell line.

Antibody arrays. Cell lysates (1 ml) were incubated overnight with antibody array membranes, using a human MMP antibody array kit (Abcam, Cambridge, MA, USA). The membranes were washed and incubated with a secondary biotin-conjugated antibody, followed by incubation with horseradish peroxidase–conjugated streptavidin, according to the manufacturer's direction. The arrays were developed, using enhanced chemiluminescence, and imaged on the ChemiDoc Imaging System (BioRad, Hercules, CA, USA). Labeling of each protein in the array was quantified using ImageJ software (NIH—http://rsbweb.nih.gov/ij/). The mean of six negative controls was subtracted for background correction, and the mean of six positive controls was used to normalize the data and calculate the relative expression levels.

Western blotting. Western blots were performed as previously described.[16] Briefly, cellular lysates, or recombinant proMMP2 or proMMP9 (R&D Systems), were diluted in SDS sample buffer containing 5% β-mercaptoethanol, run on precast 4%–20% Tris-HCl gradient gels (BioRad), and blotted with antibodies against MMP2, MMP9, HIF1A (R&D Systems), HIF2A/EPAS1 (Novus Biologicals, Littleton, CO, USA), β-actin (Cell Signaling) and HSPA6 (Abcam) diluted 1 : 1000 in TTBS and 5% milk. Densitometry was used to quantify gray levels of protein bands of interest, using image analysis software (SimplePCI, Hamamatsu). Background gray levels, determined in a blank lane, were subtracted to obtain the specific gray level for each band. Values for proteins of interest were divided by values for the loading controls (β-actin) before comparison.

ELISA. Cells were cultured and treated in six-well plates. ELISA was conducted in duplicate, using HBEGF, MMP2, HIF1A and HIF2A DuoSet ELISA Development kits (R&D Systems). The optical density of the final reaction product was determined at 450 nm using a programmable multiplate spectrophotometer (Power Wave Workstation; Bio-Tek Instruments, Winooski, VT, USA) with automatic wavelength correction. Data are presented as nanograms (ng) of HBEGF HIF1A, HIF2A, or MMP2 per microgram (μg) of total protein, determined using standard curves generated with the respective recombinant proteins (R&D Systems).

Immunocytochemistry. Immunohistochemistry was performed using a DAKO (Carpinteria, CA, USA) Autostainer Universal Staining System, as previously described.[56] Rehydrated sections of cultured explants were labeled for 1 h at 25 °C with 5 μg/ml goat polyclonal antibody against MMP2 and human recombinant HBEGF (R&D Systems) that recognizes both membrane and secreted forms of the protein and 2.5 μg/ml antibody against cytokeratin (CK7) specific for TB and counterstained with hematoxylin. Controls were incubated with 10 μg/ml non-immune goat IgG (Jackson Immunoresearch Laboratories, West Grove, PA, USA). Tissues were then incubated 1 h at 25 °C with 0.1 μg/ml rabbit anti-goat IgG (Jackson Immunoresearch). Slides were viewed at 400× magnification using a Leica (Wetzlar, Germany) DM IRB inverted microscope and imaged with spot camera.

HTR-8/SVneo cells cultured in 96-well plates were labeled with monoclonal antibodies against HBEGF (R&D Systems) diluted 1 : 500, MMP2 (R&D Systems) diluted 1 : 200, HSPA1A (Abcam) diluted 1 : 400, or HSPA6 (Abcam) diluted 1 : 400, HIF1A and HIF2A (R&D Systems) diluted 1: 200. To visualize and quantify bound primary antibody, an Envision System peroxidase anti-mouse/rabbit kit (DAKO) was used. Staining (gray level) was imaged using a Leica DM IRB epifluorescence microscope, and images were captured using a Hamamatsu Orca digital camera, or a Spot Jr. (Diagnostic Instrument Inc., Sterling Heights, MI, USA) color digital camera. Images were semi-quantified from triplicate wells in each experiment using SimplePCI (Hamamatsu) imaging software, as previously described.[56]

TUNEL. Cell death based on DNA fragmentation was quantified using the TUNEL method. Cells or tissue sections prepared for immunohistochemistry were assayed using a fluorescein-based cell death detection kit (Roche Applied Science, Indianapolis, IN, USA) according to the manufacturer's instructions. Images were captured from triplicate wells in each experiment, as described for immunocytochemistry.

qPCR. RNA from HTR-8/SVneo cells was collected using the miRNeasy kit (Qiagen, Germantown, MD, USA), according to the manufacturer's protocol. RNA concentration was determined using the NanoDrop spectrophotometer and purity was ascertained with a microfluidic Bioanalyzer (Agilent Technologies—2100 Electrophoresis Bioanalyzer Instrument). RNA was used in subsequent qPCR[57] analysis. Reverse transcription was performed using the Quantitect Reverse Transcription kit (Qiagen), and qPCR for MMP2, HBEGF and HSPA6 was conducted in triplicate with the Quantitect SYBR Green PCR kit without UNG (Qiagen), in a final volume of 25 μl. GAPDH and SDHA were used as housekeeping gene to normalize the data. Semi-quantiative analysis was performed according to the $\Delta\Delta$Ct method.[58] Primers for GAPDH, SDHA, HBEGF, MMP2 and HSPA6 were obtained from Qiagen.

Proximity ligation assay. PLA was performed in situ using Duolink In Situ Red Starter Kit Mouse/Rabbit kit (Sigma-Aldrich) according the manufacturer instruction. Briefly, following the treatment, HTR-8/SVneo cells were fixed, permeabilized and dual labeled with primary antibodies for HSPA6 and MMP2, HSPA6 and HBEGF, MMP2 and HBEGF in pre-blocking buffer (0.05% Triton X-100 in PBS, pH 7.4) overnight at 4 °C. A negative control was also included in this experiment by incubating the cells in blocking solution without primary antibodies. Next, cells were washed and incubated with rabbit plus and mouse minus PLA probes for 60 min at 37 °C. After a brief wash, the ligation ligase mixture was added and cells were incubated for another 30 min at 37 °C followed by an amplification step where adding the amplification-polymerase solution generates a rolling DNA circle. Hoechst 33342 was used to stain nuclei. The fluorescently labeled oligonucleotides were visualized by a Nikon Eclipse 90i epifluorescence microscope (Nikon Inc., Melville, USA).

HIF1A and HIF2A knockdown. HTR-8/SVneo cells were transfected in a 6-well plate (110 000 per well) for 48 h with four siRNAs that target bothe HIF1A (SAS1_Hs01_00122700, 00122702, 00122705, SAS1_Hs02_00332065; Sigma-Aldrich) and HIF2A (SAS1_Hs02_00331832, 00331833, SAS1_Hs01_00019159, SAS1_Hs01_00019157; Sigma-Aldrich). Controls included no transfection, transfection with a scrambled siRNA (Sigma-Aldrich). Based on preliminary experiments, 50 pM siRNA was chosen for all knockdown. Knockdown was analyzed using ELISA for HIF1A and HIF2A.

LongRNA library prep for next-generation sequencing. LongRNA was isolated using the miRNeasy mini kit (Qiagen). The RNA was quantified and its purity assessed with an Agilent 2100 Electrophoresis Microfluidics Analyzer. RNA was converted into an adapter-ligated cDNA library, using Ovation & Encore Library Preparation Kit (NuGen), according to the manufacture's protocol. Each cDNA sample was bar-coded, and the resulting 12 libraries (three replicate libraries for each of the four O_2 conditions) were combined for next-generation sequencing. Paired-end sequencing was performed for 50 cycles using the Illumina HiSeq-2500 sequencer.

Data alignment and mapping. RNA sequencing data was first processed with demultiplexing software (Casava 1.8.2, Illumina , San Diego, CA, USA). It was then aligned to the human genome build HG19, and to the ribosomal sequences 18 s and 28 s, using bioinformatics tool Novoalign (Novocraft, 2010). Novoalign determined unique alignments that were used to generate 1000 reads per coding segment per sample. The reads thus generated were converted into bed.files and imported to the Genomatix mapping station (Genomatix Software GmbH). The Genomatix (Ann Arbor, MI, USA) mapping station, using RNA-seq analysis, generated data in the form of Reads Per Kilobase of exon per Million fragments mapped (RPKM) for 25 000 genes in the database.

Promoter extraction. The Genomatix Genome Analyzer (GGA) MatInspector program[59] was used to extract the promoter regions for the differentially regulated genes.

Statistics. All statistics were performed with GraphPad (La Jolla, CA, USA) Prism 6 software. One-way ANOVA with Student–Newman–Keuls *post hoc* comparisons was used to identify changes between controls and treatments. Two-way ANOVA was used for experiments with multiple groups. Significance was defined as $P<0.05$; all experiments were done three times ($n=3$) using triplicate sampling, and data are expressed as mean $\pm$ S.D.

Data and materials availability. Sequencing data are available from Dryad Digital Repository at http://dx.doi.org/10.5061/dryad.4b7q9.

Conflict of Interest

The authors declare no conflict of interest.

Acknowledgements. We thank Northland Family Planning Centers of Michigan and their patients for participating in this research study. The authors are grateful to Anelia Petkova for technical assistance, and to Dr. Stephen A. Krawetz, Dr. Susan Dombrowski, Robert Goodrich, and Edward Sendler for training in next-generation sequencing library preparation and bioinformatics. This research was supported by NIH grant HD071408.

Author contributions

The study and experimental design was conceived by DRA. CVJ, PJ, CTB, ADB and BAK performed the experiments and contributed to data analysis. CVJ and DRA wrote the manuscript. MH provided placental tissue. All authors discussed the results and contributed modifications of the manuscript.

1. Burton GJ. Oxygen, the Janus gas; its effects on human placental development and function. *J Anat.* 2009; **215**: 27–35.
2. Armant DR, Kilburn BA, Petkova A, Edwin SS, Duniec-Dmuchowski ZM, Edwards HJ *et al.* Human trophoblast survival at low oxygen concentrations requires metalloproteinase-mediated shedding of heparin-binding EGF-like growth factor. *Development* 2006; **133**: 751–759.
3. Fritz R, Jain C, Armant DR. Cell signaling in trophoblast-uterine communication. *Int J Dev Biol* 2014; **58**: 261–271.
4. Jessmon P, Kilburn BA, Romero R, Leach RE, Armant DR. Function-specific intracellular signaling pathways downstream of heparin-binding EGF-like growth factor utilized by human trophoblasts. *Biol Reprod* 2010; **82**: 921–929.
5. Armant DR, Fritz R, Kilburn BA, Kim YM, Nien JK, Maihle NJ *et al.* Reduced expression of the epidermal growth factor signaling system in preeclampsia. *Placenta* 2015; **36**: 270–278.
6. Leach RE, Romero R, Kim YM, Chaiworapongsa T, Kilbum B, Das SK *et al.* Pre-eclampsia and expression of heparin-binding EGF-like growth factor. *Lancet* 2002; **360**: 1215–1219.
7. Loffek S, Schilling O, Franzke CW. Series "matrix metalloproteinases in lung health and disease": Biological role of matrix metalloproteinases: a critical balance. *Eur Respir J* 2011; **38**: 191–208.
8. Stamenkovic I. Extracellular matrix remodelling: the role of matrix metalloproteinases. *J Pathol* 2003; **200**: 448–464.
9. Staun-Ram E, Shalev E. Human trophoblast function during the implantation process. *Reprod Biol Endocrinol* 2005; **3**: 56.
10. Jovanovic M, Stefanoska I, Radojcic L, Vicovac L. Interleukin-8 (CXCL8) stimulates trophoblast cell migration and invasion by increasing levels of matrix metalloproteinase (MMP)2 and MMP9 and integrins alpha5 and beta1. *Reproduction* 2010; **139**: 789–798.
11. Chow FL, Fernandez-Patron C. Many membrane proteins undergo ectodomain shedding by proteolytic cleavage. Does one sheddase do the job on all of these proteins?. *IUBMB Life* 2007; **59**: 44–47.
12. Cheng CY, Tseng HC, Yang CM. Bradykinin-mediated cell proliferation depends on transactivation of EGF receptor in corneal fibroblasts. *J Cell Physiol* 2012; **227**: 1367–1381.
13. Roelle S, Grosse R, Aigner A, Krell HW, Czubayko F, Gudermann T. Matrix metalloproteinases 2 and 9 mediate epidermal growth factor receptor transactivation by gonadotropin-releasing hormone. *J Biol Chem* 2003; **278**: 47307–47318.
14. Torres CG, Pino AM, Sierralta WD. A cyclized peptide derived from alpha fetoprotein inhibits the proliferation of ER-positive canine mammary cancer cells. *Oncol Rep* 2009; **21**: 1397–1404.
15. Graham CH, Hawley TS, Hawley RG, MacDougall JR, Kerbel RS, Khoo N *et al.* Establishment and characterization of first trimester human trophoblast cells with extended lifespan. *Exp Cell Res* 1993; **206**: 204–211.
16. Kilburn BA, Wang J, Duniec-Dmuchowski ZM, Leach RE, Romero R, Armant DR. Extracellular matrix composition and hypoxia regulate the expression of HLA-G and integrins in a human trophoblast cell line. *Biol Reprod* 2000; **62**: 739–747.
17. Genbacev O, Schubach SA, Miller RK. Villous culture of first trimester human placenta–model to study extravillous trophoblast (EVT) differentiation. *Placenta* 1992; **13**: 439–461.
18. Castellucci M, Kaufmann P, Bischof P. Extracellular matrix influences hormone and protein production by human chorionic villi. *Cell Tissue Res* 1990; **262**: 135–142.
19. Lindell TJ, Weinberg F, Morris PW, Roeder RG, Rutter WJ. Specific inhibition of nuclear RNA polymerase Ii by alpha-amanitin. *Science* 1970; **170**: 447–449.
20. Jiang BH, Zheng JZ, Leung SW, Roe R, Semenza GL. Transactivation and inhibitory domains of hypoxia-inducible factor 1alpha. Modulation of transcriptional activity by oxygen tension. *J Biol Chem* 1997; **272**: 19253–19260.

21. Schlecht R, Scholz SR, Dahmen H, Wegener A, Sirrenberg C, Musil D *et al.* Functional analysis of Hsp70 inhibitors. *PloS One* 2013; **8**: e78443.
22. Tavaria M, Gabriele T, Kola I, Anderson RL. A hitchhiker's guide to the human Hsp70 family. *Cell Stress Chaperones* 1996; **1**: 23–28.
23. Onogi A, Naruse K, Sado T, Tsunemi T, Shigetomi H, Noguchi T *et al.* Hypoxia inhibits invasion of extravillous trophoblast cells through reduction of matrix metalloproteinase (MMP)-2 activation in the early first trimester of human pregnancy. *Placenta* 2011; **32**: 665–670.
24. Jain CV, Jessmon P, Kilburn BA, Jodar M, Sendler E, Krawetz SA *et al.* Regulation of HBEGF by micro-RNA for survival of developing human trophoblast cells. *PloS One* 2016; **11**: e0163913.
25. Brosens IA, Robertson WB, Dixon HG. The role of the spiral arteries in the pathogenesis of preeclampsia. *Obstet Gynecol Annu* 1972; **1**: 177–191.
26. DiFederico E, Genbacev O, Fisher SJ. Preeclampsia is associated with widespread apoptosis of placental cytotrophoblasts within the uterine wall. *Am J Pathol* 1999; **155**: 293–301.
27. Redman CW, Sargent IL. Latest advances in understanding preeclampsia. *Science* 2005; **308**: 1592–1594.
28. Wang GL, Semenza GL. General involvement of hypoxia-inducible factor-I in transcriptional response to hypoxia. *Nat Genet.* 1993; **90**: 4304–4308.
29. Semenza GL. Targeting HIF-1 for cancer therapy. *Nat Rev Cancer* 2003; **3**: 721–732.
30. Lisy K, Peet DJ. Turn me on: regulating HIF transcriptional activity. *Cell Death Differ* 2008; **15**: 642–649.
31. Park JK, Kang TG, Kang MY, Park JE, Cho IA, Shin JK *et al.* Increased NFAT5 expression stimulates transcription of Hsp70 in preeclamptic placentas. *Placenta* 2014; **35**: 109–116.
32. Parsell DA, Sauer RT. Induction of a heat shock-like response by unfolded protein in *Escherichia coli*: dependence on protein level not protein degradation. *Genes Dev* 1989; **3**: 1226–1232.
33. Fulda S, Gorman AM, Hori O, Samali A. Cellular stress responses: cell survival and cell death. *Int J Cell Biol* 2010; **2010**: 214074.
34. Schwarz DS, Hutvagner G, Du T, Xu Z, Aronin N, Zamore PD. Asymmetry in the assembly of the RNAi enzyme complex. *Cell* 2003; **115**: 199–208.
35. Pratt WB, Toft DO. Regulation of signaling protein function and trafficking by the hsp90/hsp70-based chaperone machinery. *Exp Biol Med* 2003; **228**: 111–133.
36. Pratt WB, Gestwicki JE, Osawa Y, Lieberman AP. Targeting Hsp90/Hsp70-based protein quality control for treatment of adult onset neurodegenerative diseases. *Annu Rev Pharmacol Toxicol* 2015; **55**: 353–371.
37. Carrigan PE, Sikkink LA, Smith DF, Ramirez-Alvarado M. Domain:domain interactions within Hop, the Hsp70/Hsp90 organizing protein, are required for protein stability and structure. *Protein Sci* 2006; **15**: 522–532.
38. Hernandez MP, Sullivan WP, Toft DO. The assembly and intermolecular properties of the hsp70-Hop-hsp90 molecular chaperone complex. *J Biol Chem* 2002; **277**: 38294–38304.
39. Wegele H, Muller L, Buchner J. Hsp70 and Hsp90–a relay team for protein folding. *Rev Physiol Biochem Pharmacol* 2004; **151**: 1–44.
40. Walsh N, Larkin A, Swan N, Conlon K, Dowling P, McDermott R *et al.* RNAi knockdown of Hop (Hsp70/Hsp90 organising protein) decreases invasion via MMP-2 down regulation. *Cancer Lett* 2011; **306**: 180–189.
41. Sims JD, McCready J, Jay DG. Extracellular heat shock protein (Hsp)70 and Hsp90alpha assist in matrix metalloproteinase-2 activation and breast cancer cell migration and invasion. *PloS One* 2011; **6**: e18848.
42. Nollen EA, Morimoto RI. Chaperoning signaling pathways: molecular chaperones as stress-sensing 'heat shock' proteins. *J Cell Sci* 2002; **115**: 2809–2816.
43. Montagnana M, Lippi G, Albiero A, Scevarolli S, Salvagno GL, Franchi M *et al.* Evaluation of metalloproteinases 2 and 9 and their inhibitors in physiologic and pre-eclamptic pregnancy. *J Clin Lab Anal* 2009; **23**: 88–92.
44. Narumiya H, Zhang YL, Fernandez-Patron C, Guilbert LJ, Davidge ST. Matrix metalloproteinase-2 is elevated in the plasma of women with preeclampsia. *Hypertens Pregnancy* 2001; **20**: 185–194.
45. Myers JE, Merchant SJ, Macleod M, Mires GJ, Baker PN, Davidge ST. MMP-2 levels are elevated in the plasma of women who subsequently develop preeclampsia. *Hypertens Pregnancy* 2005; **24**: 103–115.
46. Eleuterio NM, Palei ACT, Machado JSR, Tanus-Santos JE, Cavalli RC, Sandrim VC. Positive correlations between circulating adiponectin and MMP2 in preeclampsia pregnant. *Pregnancy Hypertens* 2015; **5**: 205–208.
47. Jirecek S, Hohlagschwandtner M, Tempfer C, Knofler M, Husslein P, Zeisler H. Serum levels of heat shock protein 70 in patients with preeclampsia: a pilot-study. *Wien Klin Wochenschr* 2002; **114**: 730–732.
48. Yung HW, Atkinson D, Campion-Smith T, Olovsson M, Charnock-Jones DS, Burton GJ. Differential activation of placental unfolded protein response pathways implies heterogeneity in causation of early- and late-onset pre-eclampsia. *J Pathol* 2014; **234**: 262–276.
49. Fukushima A, Kawahara H, Isurugi C, Syoji T, Oyama R, Sugiyama T *et al.* Changes in serum levels of heat shock protein 70 in preterm delivery and pre-eclampsia. *J Obstet Gynaecol Res* 2005; **31**: 72–77.
50. Molvarec A, Rigo J Jr., Lazar L, Balogh K, Mako V, Cervenak L *et al.* Increased serum heat-shock protein 70 levels reflect systemic inflammation, oxidative stress and hepatocellular injury in preeclampsia. *Cell Stress Chaperones* 2009; **14**: 151–159.
51. Ekambaram P. HSP70 expression and its role in preeclamptic stress. *Indian J Biochem Biophys* 2011; **48**: 243–255.
52. Liu Y, Li N, You L, Liu X, Li H, Wang X. HSP70 is associated with endothelial activation in placental vascular diseases. *Mol Med* 2008; **14**: 561–566.
53. Tamura Y, Watanabe F, Nakatani T, Yasui K, Fuji M, Komurasaki T *et al.* Highly selective and orally active inhibitors of type IV collagenase (MMP-9 and MMP-2): N-sulfonylamino acid derivatives. *J Med Chem* 1998; **41**: 640–649.
54. Rossello A, Nuti E, Orlandini E, Carelli P, Rapposelli S, Macchia M *et al.* New N-arylsulfonyl-N-alkoxyaminoacetohydroxamic acids as selective inhibitors of gelatinase A (MMP-2). *Bioorg Med Chem* 2004; **12**: 2441–2450.
55. White AR, Du T, Laughton KM, Volitakis I, Sharples RA, Xilinas ME *et al.* Degradation of the Alzheimer disease amyloid beta-peptide by metal-dependent up-regulation of metalloprotease activity. *J Biol Chem* 2006; **281**: 17670–17680.
56. Leach RE, Jessmon P, Coutifaris C, Kruger M, Myers ER, Ali-Fehmi R *et al.* High throughput, cell type-specific analysis of key proteins in human endometrial biopsies of women from fertile and infertile couples. *Hum Reprod* 2012; **27**: 814–828.
57. Bustin SA, Benes V, Garson JA, Hellemans J, Huggett J, Kubista M *et al.* The MIQE guidelines: minimum information for publication of quantitative real-time PCR experiments. *Clin Chem* 2009; **55**: 611–622.
58. Pfaffl MW. A new mathematical model for relative quantification in real-time RT-PCR. *Nucleic Acids Res* 2001; **29**: e45.
59. Cartharius K, Frech K, Grote K, Klocke B, Haltmeier M, Klingenhoff A *et al.* MatInspector and beyond: promoter analysis based on transcription factor binding sites. *Bioinformatics* 2005; **21**: 2933–2942.

Supplementary Information accompanies this paper on Cell Death and Differentiation website (http://www.nature.com/cdd)